NeuroImage xxx (2015) xxx–xxx

Contents lists available at ScienceDirect

NeuroImage

journal homepage: www.elsevier.com/locate/ynimg

Developmental synchrony of thalamocortical circuits in the neonatal brain

Joann S. Poh [a,c], Yue Li [a], Nagulan Ratnarajah [a], Marielle V. Fortier [d], Yap-Seng Chong [c,e], Kenneth Kwek [f], Seang-Mei Saw [g], Peter D. Gluckman [c,h], Michael J. Meaney [c,i,j], Anqi Qiu [a,b,c,*]

[a] Department of Biomedical Engineering, National University of Singapore, Singapore
[b] Clinical Imaging Research Centre, National University of Singapore, Singapore
[c] Singapore Institute for Clinical Sciences, Agency for Science, Technology and Research, Singapore
[d] Department of Diagnostic and Interventional Imaging, KK Women's and Children's Hospital, Singapore
[e] Department of Obstetrics and Gynaecology, Yong Loo Lin School of Medicine, National University of Singapore, National University Health System, Singapore
[f] Department of Maternal Fetal Medicine, KK Women's and Children's Hospital, Singapore
[g] Saw Swee Hock School of Public Health, National University of Singapore, Singapore, Singapore
[h] Liggins Institute, University of Auckland, Auckland, New Zealand
[i] Ludmer Centre for Neuroinformatics and Mental Health, Douglas Mental Health University Institute, McGill University, Canada
[j] Sackler Program for Epigenetics and Psychobiology, McGill University, Canada

ARTICLE INFO

Article history:
Received 31 December 2014
Accepted 14 March 2015
Available online xxxx

Keywords:
Diffusion tensor imaging
Neonatal brain
Cortical thickness
Thalamocortical connectivity
Thalamic nuclei

ABSTRACT

The thalamus is a deep gray matter structure and consists of axonal fibers projecting to the entire cortex, which provide the anatomical support for its sensorimotor and higher-level cognitive functions. There is limited *in vivo* evidence on the normal thalamocortical development, especially in early life. In this study, we aimed to investigate the developmental patterns of the cerebral cortex, the thalamic substructures, and their connectivity with the cortex in the first few weeks of the postnatal brain. We hypothesized that there is developmental synchrony of the thalamus, its cortical projections, and corresponding target cortical structures. We employed diffusion tensor imaging (DTI) and divided the thalamus into five substructures respectively connecting to the frontal, precentral, postcentral, temporal, and parietal and occipital cortex. T_2-weighted magnetic resonance imaging (MRI) was used to measure cortical thickness. We found age-related increases in cortical thickness of bilateral frontal cortex and left temporal cortex in the early postnatal brain. We also found that the development of the thalamic substructures was synchronized with that of their respective thalamocortical connectivity in the first few weeks of the postnatal life. In particular, the right thalamo-frontal substructure had the fastest growth in the early postnatal brain. Our study suggests that the distinct growth patterns of the thalamic substructures are in synchrony with those of the cortex in early life, which may be critical for the development of the cortical and subcortical functional specialization.

Introduction

The thalamocortical circuitry stems from the thalamus, a deep gray matter structure that relays and modulates information to and from the cortex. The thalamocortical circuitry undergoes rapid morphological growth to adapt to the needs of numerous sensorimotor, cognitive, and attentional functions in early life (Gilmore et al., 2012; Holland et al., 2014; Qiu et al., 2013). Thalamocortical dysconnectivity, both structural and functional, has been implicated in children with autism spectrum disorder (Nair et al., 2013), attention deficit hyperactivity disorder (ADHD; Bush, 2011; Van Ewijka et al., 2012), and schizophrenia (Jones, 1997; Woodward et al., 2012). Abnormal thalamic development has also been found in preterm infants (Ball et al., 2012; Srinivasan et al., 2007), and survivors often suffer from cognitive and behavioral deficits and have an increased risk of developing autism and ADHD (D'Onofrio et al., 2013; Delobel-Ayoub et al., 2009). It has therefore been suggested that the thalamocortical circuitry might be neural substrates for understanding the biological origin of neurodevelopmental disorders (Marlow et al., 2005; Tillman et al., 2008). Hence, establishing a baseline for normal development of the thalamocortical circuits in early life is clinically relevant to understanding which characteristics of thalamocortical development may be selectively vulnerable to injury and leads to neurodevelopmental disorders.

The development of thalamocortical connections starts prenatally and continues into the neonatal period, which has been demonstrated by histochemical studies in the human newborn cortex (Mrzljak et al., 1988). Abnormal prenatal thalamic development is associated with

* Corresponding author at: Department of Biomedical Engineering, National University of Singapore, 9 Engineering Drive 1, Block EA #03-12, Singapore 117576, Singapore. Fax: +65 6872 3069.
E-mail address: bieqa@nus.edu.sg (A. Qiu).

http://dx.doi.org/10.1016/j.neuroimage.2015.03.039
1053-8119/

changes in structural alterations of the thalamocortical white matter and affiliated cortex, suggesting a close relationship among the thalamus, cortical structures, and white matter tracts connecting them. In preterm infants, reduced thalamic volume was found to be correlated with reductions in both the microstructure of the thalamic radiations (afferents to the cortex) and the cortical volume (Ball et al., 2012). This suggests a possibility that tissue volume in the thalamus and cortex reflects the thalamocortical connectivity, and is dependent on the growth and integrity of the white matter tracts connecting them. The mediodorsal thalamic volume has been implicated in schizophrenia neuropathology, and it has been speculated that decreases in its activity during early development, before the age of 2 years, could result in a loss of synaptic drive to the prefrontal cortex, leading to a decrease in prefrontal synaptic density (Ferguson & Gao, 2015; Huttenlocher, 1979). This hypoinnervation may underlie possible mechanisms of cortical gray matter reductions that have been observed in schizophrenic patients in adulthood. In addition, previous diffusion tensor imaging (DTI) studies showed that an increase in fractional anisotropy (FA) and decreases in axial diffusivity (AD) and radial diffusivity (RD) in the thalamus is in parallel with an increase FA in thalamic radiations, major white matter tracts for the thalamocortical connection (Aeby et al., 2009; Qiu et al., 2013). Altogether, there seems to be synchronous development among the thalamus, cortex, and their connectivity.

Currently, understanding the normal development of the thalamus in early life is limited as thalamic size is largely assessed using traditional methods such as T1-weighted and/or T2-weighted magnetic resonance imaging (MRI) and its microstructure is largely assessed using DTI. However, the thalamus is a fairly complicated structure and consists of axonal fibers projecting to the entire cortex, which provide the anatomical support for its numerous functions, including sensory and motor functions, as well as high-level cognition (Sherman, 2007). Based on the pattern of this widespread thalamocortical connections, the thalamus can be further divided into substructures that are composed of nuclei clusters (Herrero et al., 2002; Sim et al., 2006). However, there is limited *in vivo* evidence on the normal development of individual thalamic substructures, partly because of the lack of any distinction on their appearance on T1- and T2-weighted MRI data. Moving beyond early structural imaging studies on size, investigations of the thalamus can also be benefited by using other imaging-based methods such as DTI. Behrens et al. (2003) showed that using DTI tractography classification of the thalamic gray matter, based on the thalamocortical connectivity patterns, have revealed distinct substructures whose locations correspond to thalamic nuclei described previously in histological studies.

In this study, we aimed to investigate the developmental patterns of the cerebral cortex in terms of cortical thickness, as well as the thalamic substructures and their respective connectivity with the cortex in the first few weeks of the postnatal brain. We employed DTI and divided the thalamus into 5 substructures respectively connecting to the frontal, precentral, postcentral, temporal, and parietal and occipital cortex. The cortical development was characterized by cortical thickness assessed using T2-weighted MRI. The thalamocortical connectivity was measured using DTI. Based on the aforementioned findings, we therefore hypothesized that even shortly after birth, the growth pattern of the thalamic substructures is parallel to that of their respective thalamocortical connectivity and corresponding cortical structures.

Materials and methods

Subjects

One-hundred and eighty-nine infants of mothers who participated in the prospective GUSTO birth cohort study were recruited for neuroimaging. The GUSTO cohort consisted of pregnant Asian women attending the first trimester prenatal ultrasound scan clinic at the National University Hospital (NUH) and KK Women's and Children's Hospital (KKH) in Singapore. The parents were Singapore citizens or Permanent Residents of Chinese, Malay, or Indian ethnic background. Mothers on chemotherapy, psychotropic drugs, or with type I diabetes mellitus were excluded. Only women who agreed to donate birth tissues including cord, placenta, and cord blood at delivery were included. The cohort inclusion and exclusion criteria were described in Soh et al. (2014). The GUSTO cohort study was approved by the National Healthcare Group Domain Specific Review Board (NHG DSRB) and the SingHealth Centralized Institutional Review Board (CIRB). Written consent was obtained from mothers. Birth outcome and pregnancy measures were obtained from hospital records. This study included neonates whose postmenstrual age was of at least 35 weeks, birth weight equal or larger than 2500 g, and a minimum 5-minute APGAR score of 9.

MRI acquisition

At 5 to 17 days of life, neonates underwent fast spin-echo T2-weighted MRI and single-shot echo-planar DTI images using a 1.5-Tesla GE scanner at the Department of Diagnostic and Interventional Imaging of the KKH. The images were acquired when subjects were sleeping in the scanner. No sedation was used and precautions were taken to reduce exposure to the MRI scanner noise. A neonatologist was present during each scan session. A pulse oximeter was used to monitor heart rate and oxygen saturation throughout the entire session.

The imaging protocols included (i) fast spin-echo T2-weighted MRI (TR = 3500 ms; TE = 110 ms; FOV = 256 mm × 256 mm; matrix size = 256 × 256) and (ii) single-shot echo-planar DTI (TR = 7000 ms; TE = 56 ms; flip angle = 90°, FOV = 200 mm × 200 mm; matrix size = 64 × 64). For T2-weighted MRI, 50 axial slices with 2.0 mm thickness were acquired parallel to the anterior–posterior commissure line. Two T2-weighted images were acquired per subject. For DTI, 40 to 50 axial slices with 3.0 mm thickness were acquired parallel to the anterior–posterior commissure line. Nineteen diffusion-weighted images (DWIs) with b = 600 s/mm^2 and 1 baseline with b = 0 s/mm^2 were also obtained.

All 189 neonates had the T2-weighted MRI data, while only 142 neonates had the DTI data. Through visual inspection, only 122 neonates had a good DTI data, partially because DTI was last acquired and sensitive to head motion.

Cortical thickness analysis

Within individual subjects, when possible, two T2-weighted MRI acquisitions were first rigidly aligned and averaged to increase signal-to-noise ratio. In cases where only one scan was acquired, data from one scan was used in lieu of the average axial image. The skull of the averaged axial image was removed using Brain Extraction Tool (BET; Smith, 2002). A Markov random field model (MRF) was used to automatically delineate gray matter, white matter, and cerebrospinal fluid (CSF) from the neonatal T2-weighted MRI data. The mathematical model of MRF was detailed in Fischl et al. (2002). The MRF model has been considered as one of robust automatic brain segmentation approaches because it incorporates the anatomical prior information obtained from a manually labeled training set. In our study, our training set consisted of twenty T2-weighted MRI data sets randomly selected from our sample. We employed the leave-one-out validation approach to evaluate the MRF segmentation accuracy for gray matter and white matter. The nineteen images with the manual label were used as training sets in MRF and one image with the manual label was used as a testing set. The accuracies of the MRF segmentation for gray and white matter were respectively 0.793 and 0.862.

Based on the above tissue segmentation, a cortical surface was constructed at the boundary between gray and white matter using graph-based topology correction algorithm (Han et al., 2002). The cortical thickness was measured as the distance between the cortical surface and gray matter voxels at the boundary between gray matter and CSF.

Please cite this article as: Poh, J.S., et al., Developmental synchrony of thalamocortical circuits in the neonatal brain, NeuroImage (2015), http://dx.doi.org/10.1016/j.neuroimage.2015.03.039

The cortical thickness was smoothed using the Laplace-Beltrami basis functions on the cortical surface. For group comparison of the cortical thickness, we employed a large deformation diffeomorphic metric mapping (LDDMM) algorithm (Zhong & Qiu, 2010) to align individual cortical surfaces to the atlas that was generated based on the cortical anatomy of the same twenty subjects (Bai et al., 2012; Joshi et al., 2004) and transferred the thickness of each individual subject to the atlas.

Thalamus and its substructure delineation

Preprocessing

The thalamus delineation from T2-weighted images and its accuracy were reported in our previous study (Qiu et al., 2013). DTI data were preprocessed as described previously (Qiu et al., 2013). Briefly, as shown in Fig. 1A, within individual subjects, DWIs were corrected for motion and eddy current distortions using affine transformation to the image without diffusion weighting using FSL. Six elements of the diffusion tensor were then determined using FSL, from which FA, AD, and RD were calculated. The thalamus masks in the T2-weigted image were then superimposed to the DWI, FA, AD, and RD images through rigid transformation obtained between the image without diffusion weighting and T2-weighted image using FSL. The LDDMM algorithm was employed to align individual subjects' DTI to the GUSTO DTI atlas (see details of the GUSTO atlas in Bai et al., 2012).

Atlas set generation

The thalamus was further delineated into five substructures according to their connections with the frontal, precentral, postcentral, parietal, and occipital, and temporal cortices (Fig. 2) using a weighted multi-atlas label fusion method (Artaechevarria et al., 2009). As shown in Fig. 1B, we first constructed the atlas set that contains 20 DTI data sets randomly chosen from the GUSTO cohort. For each DTI atlas data set, probabilistic fiber tracking (1000 tracts per voxel) was performed from the left and right thalamic regions separately (Parker et al., 2003). The probabilities of each thalamic voxel connecting to the five cortical regions were computed as the ratio of fibers connecting them to the total number of fibers. Every thalamic voxel was then labeled with the corresponding cortical segment with the highest probability score. This atlas set was then used in the weighted multi-atlas label fusion method to automatically delineate the five thalamic substructures (frontal, precentral, postcentral, parietal and occipital, and temporal thalamic substructures).

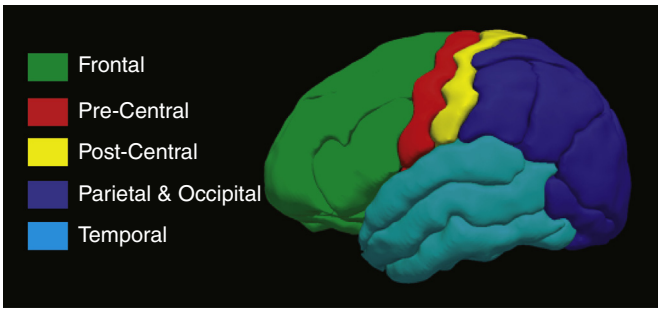

Fig. 2. Cortical parcellation.

Weighted multi-atlas label fusion method

Denote $D(x)$ as the diffusion tensor of a subject at location x, where x is the coordinate of a voxel in the atlas space. Denote $D_i(x)$ and $L_i(x)$, respectively, as the diffusion tensor and label of the ith atlas data at location x, where $i = 1, 2, \ldots, 20$. We computed the invariant Log-Euclidean distance metric (Arsigny et al., 2006) between $D(x)$ and $D_i(x)$ in the form of

$$d_i(x) = \| \log(D(x)) - \log(D_i(x)) \|_F = \sqrt{\text{trace}[\log(D(x)) - \log(D_i(x))]^2}. \quad (1)$$

The label of $D(x)$, $L(x)$, can be computed based on

$$L(x) = \max_{l=\{1,2,3,4,5\}} \sum_{i=1}^{5} w_i(x) 1_{\{L_i(x)=l\}}, \quad (2)$$

where $1_{\{L_i(x)=l\}}$ is an indicator function that takes value of 1 when $L_i(x)$ is equal to l. $w_i(x)$ is defined as weight estimated through

$$w_i(x) = \frac{1}{Z(x)} e^{-\frac{d_i(x)^2}{2\sigma^2}}.$$

$Z(x)$ is a normalization term such as $\sum_{i=1}^{5} w_i(x) = 1$.

We employed the leave-one-out validation procedure to evaluate the segmentation accuracy using the 20 atlases. The segmentation accuracy of the thalamic substructures, measured using volume overlap percentage (VOP), ranges from 70% to 88%, and its average across all the five thalamic substructures was 76%.

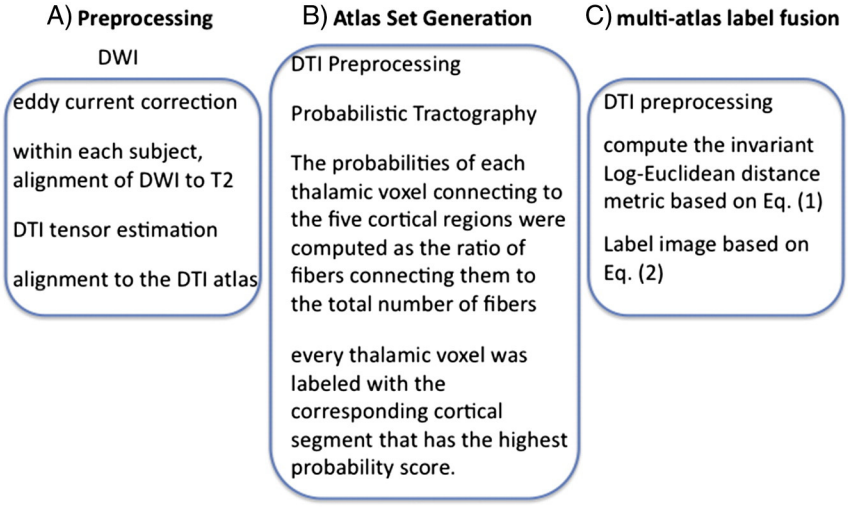

Fig. 1. A flow chart of DTI analysis.

Please cite this article as: Poh, J.S., et al., Developmental synchrony of thalamocortical circuits in the neonatal brain, NeuroImage (2015), http://dx.doi.org/10.1016/j.neuroimage.2015.03.039

Fig. 3 illustrates the segmentation results of five subjects. The mask of the thalamic substructures of individual subjects was transformed back to the subjects' space and was used to compute the substructures' volumes. The mean values of FA, AD, and RD were computed within each thalamic substructure for individual subjects. In addition, the connectivity of the thalamic substructures with the cortical regions was also

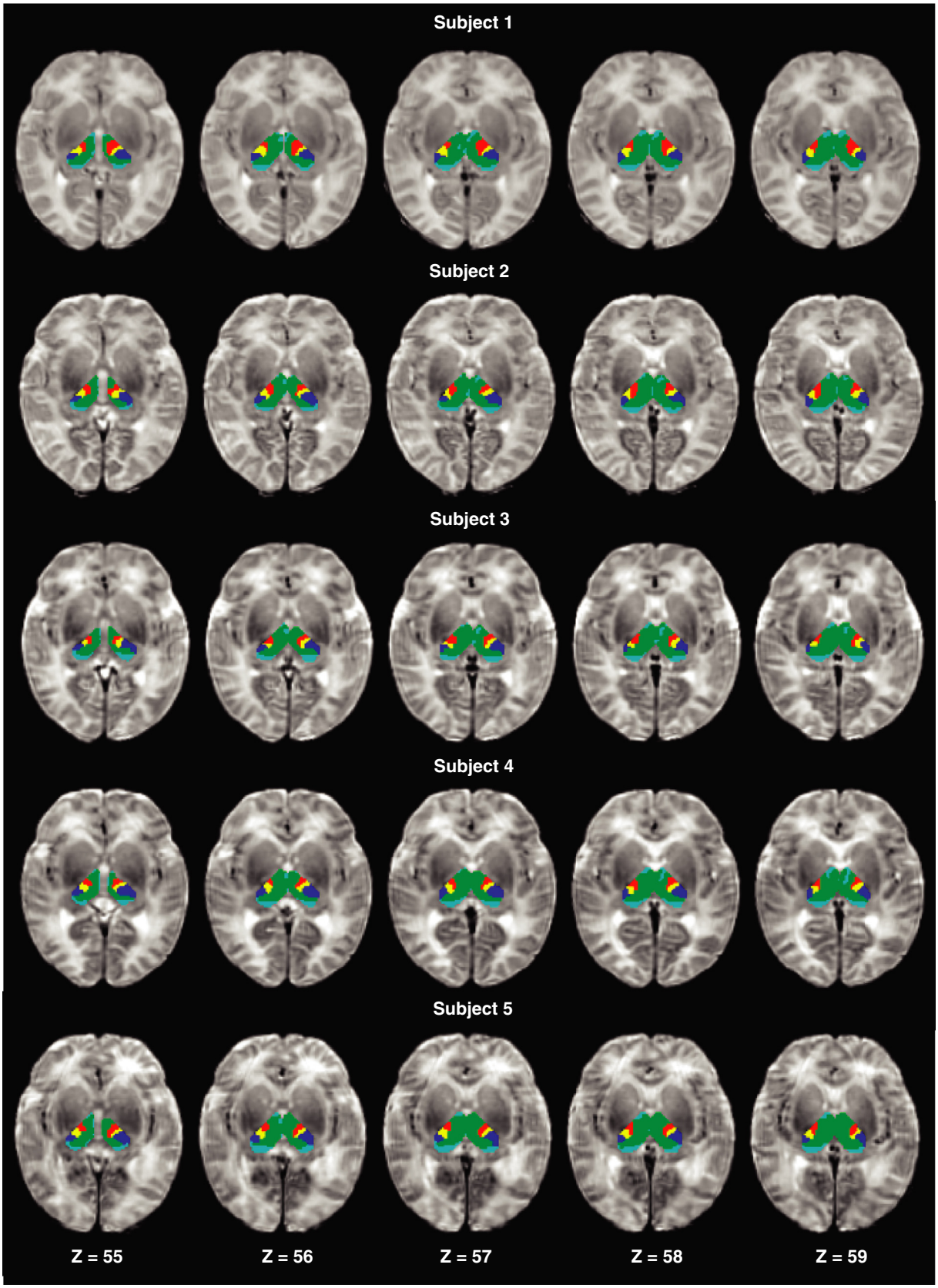

Fig. 3. Thalamic parcellation of five subjects. Each row illustrates axial slices of one subject.

Please cite this article as: Poh, J.S., et al., Developmental synchrony of thalamocortical circuits in the neonatal brain, NeuroImage (2015), http://dx.doi.org/10.1016/j.neuroimage.2015.03.039

computed based on the mean values of FA, AD, and RD within the masks containing fibers connecting between the thalamic substructures and their corresponding cortical regions. These masks were generated based on the 20 atlas DTI data sets and their probabilistic tractography in the atlas space.

Statistical analysis

Student's *t*-test was used to examine gender differences in the gestational age, postmenstrual age at the MRI visit, and birth weight.

Linear regressions were fused to examine the developmental pattern of cortical thickness in the early postnatal life using SurfStats software (Chung et al., 2010). Postmenstrual age at the MRI visit was included as a main factor. Gender, ethnicity, and birth weight adjusted for gestational age were included as covariates in the regression model. Statistical results at each surface vertex were corrected for multiple comparisons at the cluster level of significance ($p < 0.05$). The significance of each cluster was determined based on random field theory given in Chung et al. (2010).

Linear regression was further performed to examine the effect of postmenstrual age on structural volumes and DTI measures of the thalamic substructures and their connectivity. Gender, ethnicity, and birth weight adjusted for gestational age were included as covariates in the regression model. Bonferroni correction was used for the adjustment of the p-value for individual MRI measurements and hence the level of significance for individual tests was 0.005 (5 thalamic substructures and both cerebral hemispheres).

Results

Sample and demographic characteristics

Among the 122 subjects with good DTI data, this study further excluded subjects who had birth weight less than 2500 g ($n = 5$), gestational age less than 35 weeks ($n = 0$), and APGAR score less than 9 ($n = 2$). In addition, subjects whose thalamic substructures were beyond 3 deviations from their mean values were excluded ($n = 15$), as well as those with analysis errors ($n = 9$). Hence, the final study sample for the thalamus substructures included 49 males and 42 females ($n = 91$).

The ethnic composition was 37 Chinese, 38 Malays, and 16 Indians. The mean postmenstrual age at the MRI visit was 38.63 (standard deviation, SD = 1.21) weeks. There were no gender differences in the gestational age at birth (male, 38.45 ± 1.231 weeks; female, 38.85 ± 1.150 weeks; $p = 0.111$), postmenstrual age at the MRI visit (male, 39.86 ± 1.241 weeks; female, 40.25 ± 1.234 weeks; $p = 0.142$), birth weight (male, 3173.16 ± 362.038 g; female, 3104.02 ± 356.563 g; $p = 0.363$), or ethnicity ($p = 0.930$).

Developmental pattern of cortical thickness

There is a main effect of postmenstrual age on cortical thickness. Fig. 4 illustrates age-related increases in cortical thickness in bilateral frontal cortex and left temporal cortex of the early postnatal brain, especially in bilateral frontal pole, ventromedial prefrontal cortex (vmPFC), and anterior cingulate cortex (ACC), as well as left ventrolateral prefrontal cortex (vlPFC) and left superior temporal cortex.

Thalamic and thalamocortical development

As shown in Table 1 and Fig. 5, there was significant volumetric growth in bilateral thalamo-frontal and the left thalamo-parietal and occipital substructures with increasing age ($p < 0.005$). Interestingly, the right thalamo-frontal substructure showed greater growth than the other thalamic substructures ($p < 0.005$). As age increased, FA also increased in bilateral frontal and the right temporal substructures of the thalamus ($p < 0.005$). In parallel, AD decreased with age in all thalamic substructures except in the right thalamo-postcentral and parietal and occipital substructures ($p < 0.005$). RD also decreased with age in all thalamic substructures ($p < 0.001$).

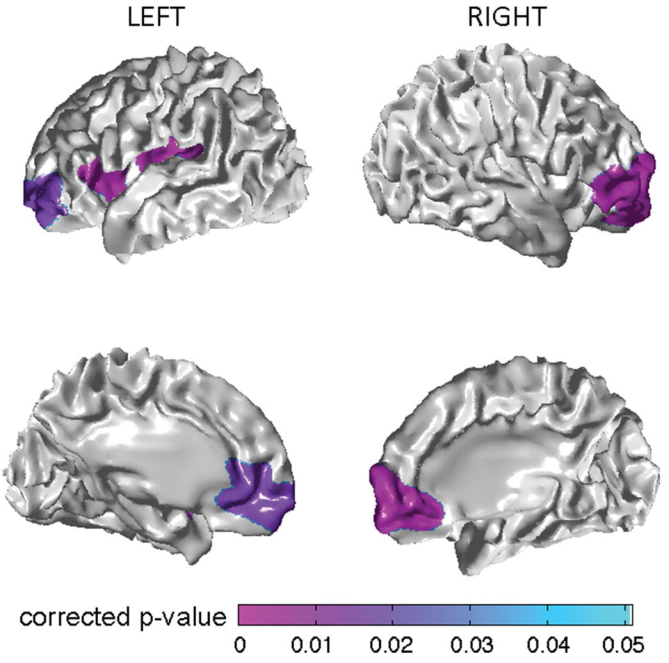

Fig. 4. Statistical map for the development of cortical thickness. The top row shows the lateral view of the cortical surface, while the bottom row shows the medial view of the cortical thickness.

The growth pattern of the thalamocortical connectivity was synchronized with that of the thalamic individual substructures in the first few weeks of the postnatal brain. As age increased, FA increased in bilateral frontal and temporal, and the left parietal and occipital white matter regions connected with the thalamus ($p < 0.005$; Table 2 and Fig. 6). There was also a decrease in AD in all but bilateral temporal, and both the left frontal and parietal and occipital regions connected to the thalamus ($p < 0.005$; Table 2 and Fig. 6). A decrease in RD was found in all but the left frontal and right temporal regions connected to the thalamus ($p < 0.005$; Table 2 and Fig. 6).

Discussion

Our study integrated the structural MRI and DTI data and demonstrated the first evidence of the development of the cortex, the thalamic

Table 1
Regional development of thalamic substructures.

Region	Hemisphere	Volume	FA	AD	RD
		β	β	β	β
Frontal	L	0.318*	0.479**	−0.519**	−0.670**
	R	0.443**	0.329*	−0.537**	−0.645**
Precentral	L	0.216	0.259	−0.478**	−0.508**
	R	0.270	0.028	−0.452**	−0.388**
Postcentral	L	0.133	0.118	−0.495**	−0.539**
	R	0.111	0.183	-0.262	−0.500**
Parietal and occipital	L	0.308*	0.206	−0.385**	−0.632**
	R	0.128	0.213	−0.206	−0.458**
Temporal	L	0.197	0.280	−0.388**	−0.501**
	R	0.183	0.364*	−0.443**	−0.572**

β is the standardized β value derived from linear regression while controlling for adjusted birth weight, gender, and ethnicity. Abbreviations: FA—fractional anisotropy; AD—axial diffusivity; RD—radial diffusivity.
* $p < 0.005$.
** $p < 0.001$.

Please cite this article as: Poh, J.S., et al., Developmental synchrony of thalamocortical circuits in the neonatal brain, NeuroImage (2015), http://dx.doi.org/10.1016/j.neuroimage.2015.03.039

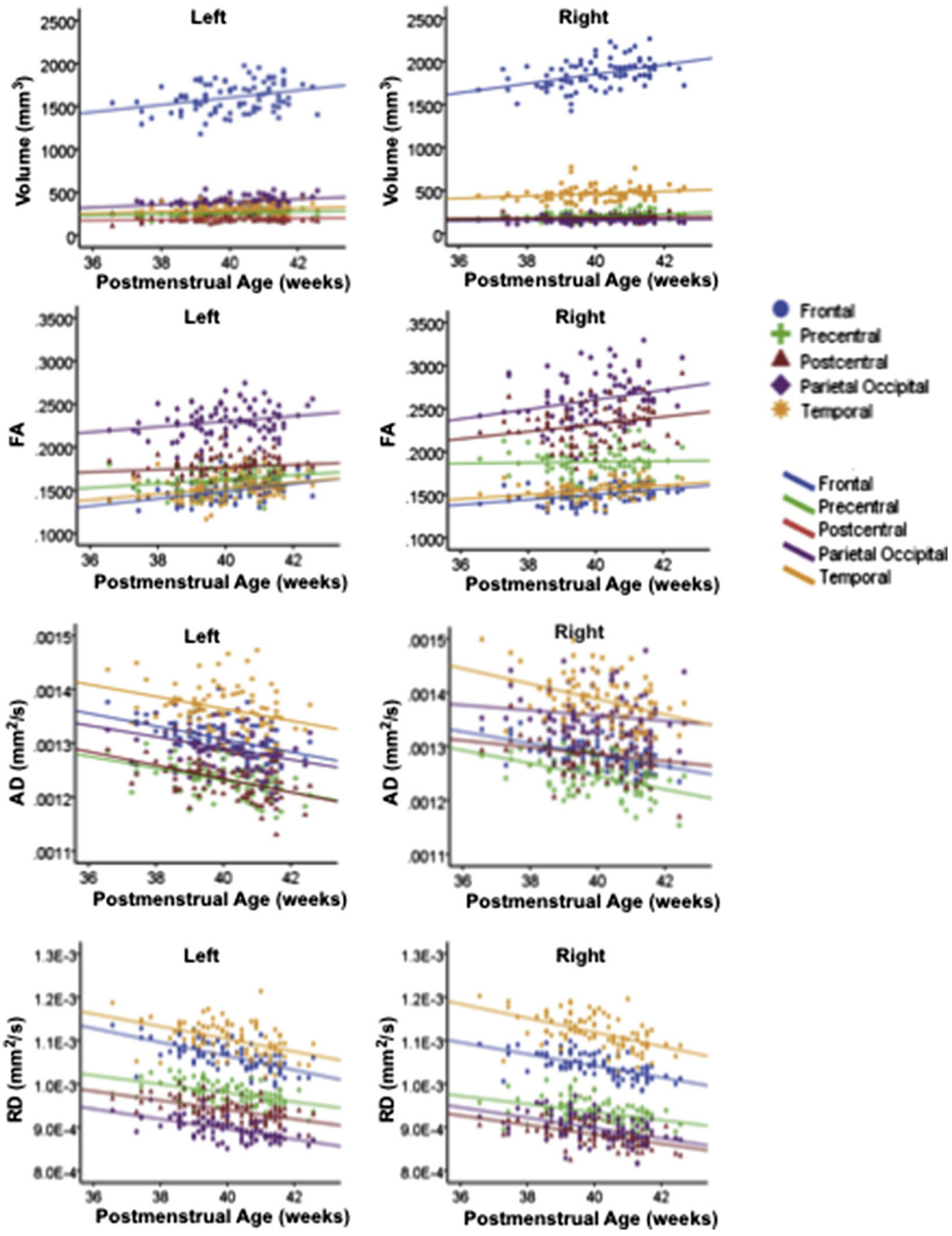

Fig. 5. Scatter plots of the volume, fractional anisotropy (FA), axial diffusivity (AD), and radial diffusivity (RD) of individual thalamic substructures against postmenstrual age.

substructures, and their connectivity in the early postnatal brain. Our study observed increases in cortical thickness of the bilateral frontal and left temporal cortices in the first few weeks of life. In addition, the development of the thalamic substructures is synchronized with that of the cortex and their corresponding thalamocortical connections in the first few weeks of the postnatal life. In particular, the right thalamo-frontal substructure had the fastest growth in the early postnatal brain.

Our study suggested the fast development of cortical thickness in the prefrontal and temporal cortex in the first few weeks of life. These findings are in line with the previous findings on the cellular and functional development of the cortex. The prefrontal cortex undergoes the largest synaptic overproduction, while the synapse elimination of the prefrontal cortex takes in place at the slowest rate in the early postnatal brain (Huttenlocher & Dabholkar, 1997; Petanjek et al., 2008, 2011). Both processes can be extended to the third decade of life. This merges with the idea that the emergence and elaboration of the prefrontal function in the human appear to occur at different ages. The functional development of the prefrontal cortex, such as executive functioning, may be gradually developed in the course of its synapse overproduction and synaptic elimination (Li et al., 2006; Zhong et al., 2014). In addition, the superior temporal cortex also undergoes synaptic overproduction and pruning in early life. However, our study suggested that the left superior temporal cortex grows even within the first few weeks of life as compared to the right, which is in line with the development of functional needs. Infants aged between birth and 10 months showed a greater sensitivity to speech stimuli in the left temporal cortex than in the right in auditory evoked responses (Molfese et al., 1975).

Please cite this article as: Poh, J.S., et al., Developmental synchrony of thalamocortical circuits in the neonatal brain, NeuroImage (2015), http://dx.doi.org/10.1016/j.neuroimage.2015.03.039

Table 2
Regional development of thalamocortical connectivity.

Region	Hemisphere	FA	AD	RD
		β	β	β
Frontal	L	0.509**	−0.177	−0.299
	R	0.547**	−0.374**	−0.533**
Precentral	L	0.257	−0.498**	−0.582**
	R	0.219	−0.488**	−0.548**
Postcentral	L	0.215	−0.508**	−0.611**
	R	0.240	−0.434**	−0.545**
Parietal and occipital	L	0.421**	−0.267	−0.491**
	R	0.272	−0.375**	−0.494**
Temporal	L	0.354*	−0.189	−0.388**
	R	0.359*	−0.027	−0.261

β is the standardized β value derived from linear regression while controlling for adjusted birth weight, gender, and ethnicity. Abbreviations: FA—fractional anisotropy; AD—axial diffusivity; RD—radial diffusivity.
* $p < 0.005$.
** $p < 0.001$.

Furthermore, our findings on the cortical thickness provided novel evidence of the brain's morphological development, adding to the existing evidence on the cortical folding pattern at the neonatal period (Hill et al., 2010). The lateral temporal and frontal cortices are highly convoluted and expanded in terms of the cortical area even at birth, which persists to later life (Hill et al., 2010). An increase in cortical thickness in the neonatal stage may be mainly due to greater synaptic overproduction than synaptic pruning. In contrast, an increase in cortical folding could be due to the dentritic length and dendritic spine density, which enhances the cortico-cortical and cortico-subcortical connections. Hence, the cortical thickness measurement adds an additional dimension for understanding the cortical morphology.

Our study supports the idea on the synchronized development of the thalamic substructures and their cortical connectivity in the early postnatal brain. In the first few weeks of life, the thalamo-frontal and thalamo-parietal and occipital substructures grow in terms of their size with potential membrane proliferation and fiber myelination, as indicated by increased FA and decreased AD and RD values (Dubois et al., 2008). Our study adds on by showing that there is also a similar growth pattern of increased FA and decreased AD and RD values in the white matter regions connecting the thalamus with the frontal, parietal, and occipital cortices. In particular, our study showed that the fastest growth occurred in the right thalamo-frontal substructure in the early postnatal brain, which was also shown in preterm infants (Eaton-Rosen et al., 2014). Furthermore, the thalamo-precentral, postcentral, and temporal substructures grew in parallel with their corresponding thalamocortical white matter regions in the first few weeks of life, albeit only in terms of

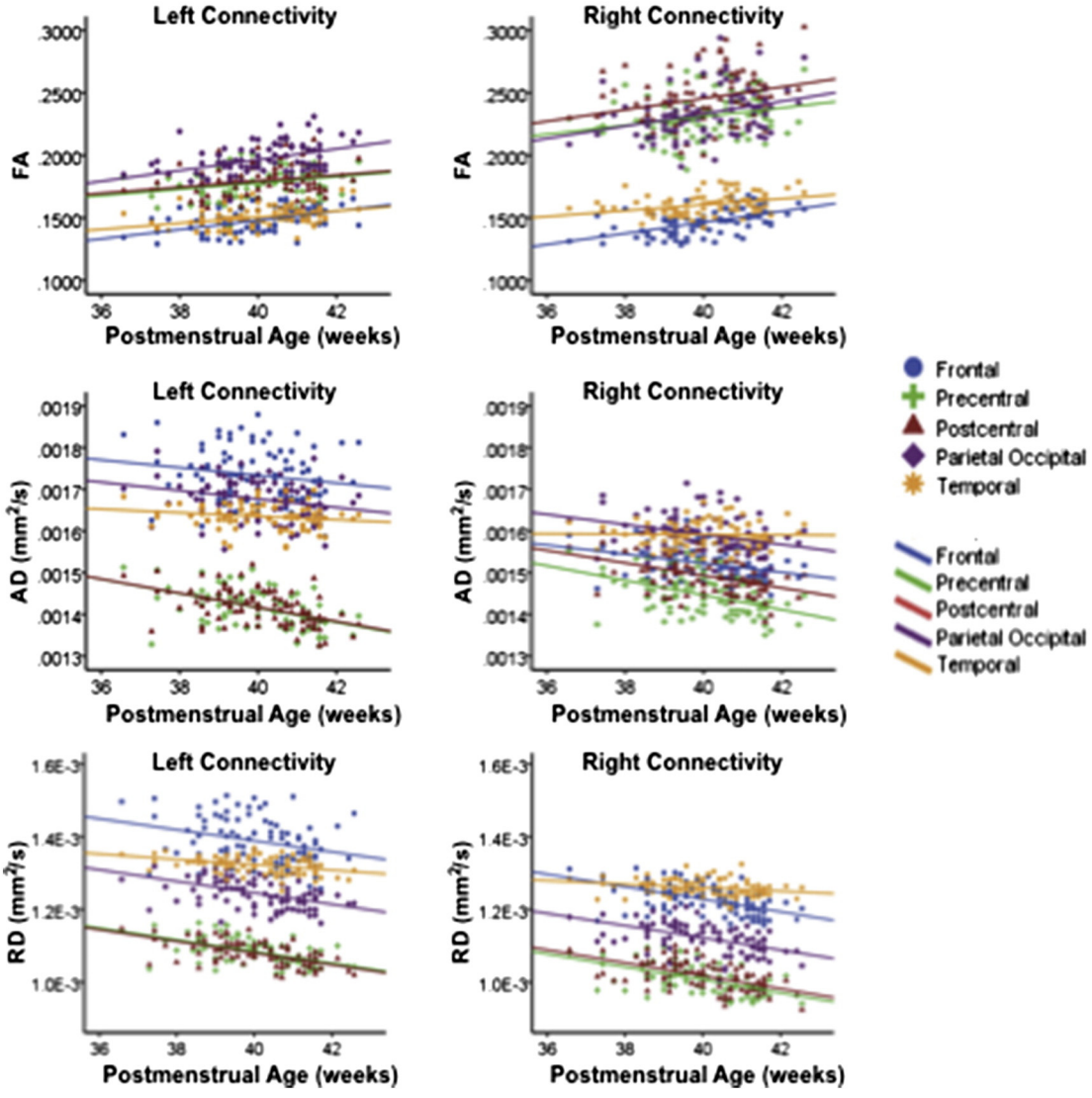

Fig. 6. Scatter plots of the fractional anisotropy (FA), axial diffusivity (AD), and radial diffusivity (RD) of individual thalamocortical connectivity against postmenstrual age.

Please cite this article as: Poh, J.S., et al., Developmental synchrony of thalamocortical circuits in the neonatal brain, NeuroImage (2015), http://dx.doi.org/10.1016/j.neuroimage.2015.03.039

potential membrane proliferation as indicated by decreased AD and RD values. Altogether, these findings are in line with evidence of the cortical development from this and previous studies, that is, the frontal and temporal cortices develop relatively more quickly than other brain regions in the early life (Gilmore et al., 2012). Together, these findings support the tension-based theory of morphogenesis proposed by van Essen, which can account for the synchronized development of different brain regions in terms of their connectivity (Hill et al., 2010; Van Essen, 1997). Our study showed that the thalamic substructures and their corresponding thalamocortical white matter regions have pronounced anisotropies in the orientation of axons and dendrites. During the cerebral growth, tension along the axons acting together pull strongly on the thalamic substructures and their corresponding cortical regions towards one another, while allowing weakly connected regions to drift apart. In addition, such distinctive thalamocortical connectivity patterns are responsible for stimulating their simultaneous growth in early life.

There are several concerns on tractographic analysis of the neonatal brain. In the neonatal brain, the white matter is largely unmyelinated and hence has low diffusion anisotropy. This could cause potential termination of fiber tracking in tractography, especially in the peripheral white matter region (region close to the cortex). To overcome this issue, our study employed the weighted multi-atlas label fusion method (Artaechevarria et al., 2009) to avoid the application of tractography on individual data sets but only on the training data sets.

In summary, this study provides the evidence on the developmental pattern of the cortex, the thalamic individual substructures, and their corresponding cortical connectivity in normal Asian neonates. The developmental pattern of the cortex in the first few weeks after birth can be characterized based on cortical thickness. In addition, the developmental pattern of the thalamic substructures in the first month after birth can be characterized as a robust increase in volume and anisotropy, as well as a decrease in both axial and radial diffusivities. The growth of the thalamic substructure is in synchrony with that of the cortex and their respective projections into the cortex. These findings are complementary with existing findings in the normal brain development of early infancy.

Acknowledgments

This research is supported by the Singapore National Research Foundation under its Translational and Clinical Research (TCR) Flagship Programme and administered by the Singapore Ministry of Health's National Medical Research Council (NMRC), Singapore; NMRC/TCR/004-NUS/2008 and NMRC/TCR/012-NUHS/2014. Additional funding is provided by the Singapore Institute for Clinical Sciences, Agency for Science Technology and Research (A*STAR), Singapore. This study is also supported by NMRC (NMRC/CBRG/0039/2013), the Young Investigator Award at the National University of Singapore (NUSYIA FY10 P07), and Singapore Ministry of Education Academic Research Fund Tier 2 (MOE2012-T2-2-130).

We thank the GUSTO study group and all clinical and home visit staff involved. The voluntary participation of all participants is greatly appreciated. The GUSTO study group includes Pratibha Agarwal, Arijit Biswas, Choon Looi Bong, Shirong Cai, Jerry Kok Yen Chan, Yiong Huak Chan, Cornelia Yin Ing Chee, Yin Bun Cheung, Audrey Chia, Amutha Chinnadurai, Chai Kiat Chng, Mary Foong-Fong Chong, Shang Chee Chong, Mei Chien Chua, Chun Ming Ding, Eric Andrew Finkelstein, Doris Fok, Keith M. Godfrey, Anne Eng Neo Goh, Yam Thiam Daniel Goh, Joshua J. Gooley, Wee Meng Han, Mark Hanson, Christiani Jeyakumar Henry, Joanna D. Holbrook, Chin-Ying Hsu, Hazel Inskip, Jeevesh Kapur, Ivy Yee-Man Lau, Bee Wah Lee, Yung Seng Lee, Ngee Lek, Sok Bee Lim, Yen-Ling Low, Iliana Magiati, Lourdes Mary Daniel, Cheryl Ngo, Krishnamoorthy Naiduvaje, Wei Wei Pang, Boon Long Quah, Victor Samuel Rajadurai, Mary Rauff, Salome A. Rebello, Jenny L. Richmond, Lynette Pei-Chi Shek, Allan Sheppard, Borys Shuter, Leher Singh, Shu-E Soh, Walter Stunkel, Lin Lin Su, Kok Hian Tan, Oon Hoe Teoh, Hugo P S van Bever, Rob M. van Dam, Inez Bik Yun Wong, P. C. Wong, Fabian Yap, George Seow Heong Yeo.

References

Aeby, A., Liu, Y., De Tiege, X., Denolin, V., David, P., Baleriaux, D., Kavec, M., Metens, T., Van Bogaert, P., 2009. Maturation of thalamic radiations between 34 and 41 weeks' gestation: a combined voxel-based study and probabilistic tractography with diffusion tensor imaging. Am. J. Neuroradiol. 30, 1780–1786.

Arsigny, V., Commowick, O., Pennec, X., Ayache, N., 2006. A log-Euclidean framework for statistics on diffeomorphisms. Medical image computing and computer-assisted intervention: MICCAI … International Conference on Medical Image Computing and Computer-Assisted Intervention 9, pp. 924–931.

Artaechevarria, X., Munoz-Barrutia, A., Ortiz-de-Solorzano, C., 2009. Combination strategies in multi-atlas image segmentation: application to brain MR data. IEEE Trans. Med. Imaging 28, 1266–1277.

Bai, J., Abdul-Rahman, M.F., Rifkin-Graboi, A., Chong, Y.S., Kwek, K., Saw, S.M., Godfrey, K.M., Gluckman, P.D., Fortier, M.V., Meaney, M.J., Qiu, A., 2012. Population differences in brain morphology and microstructure among Chinese, Malay, and Indian neonates. PLoS One 7, e47816.

Ball, G., Boardman, J.P., Rueckert, D., Aljabar, P., Arichi, T., Merchant, N., Gousias, I.S., Edwards, A.D., Counsell, S.J., 2012. The effect of preterm birth on thalamic and cortical development. Cereb. Cortex 22, 1016–1024.

Behrens, T.E., Johansen-Berg, H., Woolrich, M.W., Smith, S.M., Wheeler-Kingshott, C.A., Boulby, P.A., Barker, G.J., Sillery, E.L., Sheehan, K., Ciccarelli, O., Thompson, A.J., Brady, J.M., Matthews, P.M., 2003. Non-invasive mapping of connections between human thalamus and cortex using diffusion imaging. Nat. Neurosci. 6, 750–757.

Bush, G., 2011. Cingulate, frontal, and parietal cortical dysfunction in attention-deficit/hyperactivity disorder. Biol. Psychiatry 69, 1160–1167.

Chung, M.K., Worsley, K.J., Nacewicz, B.M., Dalton, K.M., Davidson, R.J., 2010. General multivariate linear modeling of surface shapes using SurfStat. NeuroImage 53, 491–505.

Delobel-Ayoub, M., Arnaud, C., White-Koning, M., Casper, C., Pierrat, V., Garel, M., Burguet, A., Roze, J.C., Matis, J., Picaud, J.C., Kaminski, M., Larroque, B., Group, E.S., 2009. Behavioral problems and cognitive performance at 5 years of age after very preterm birth: the EPIPAGE Study. Pediatrics 123, 1485–1492.

D'Onofrio, B.M., Class, Q.A., Rickert, M.E., Larsson, H., Långström, N., Lichtenstein, P., 2013. Preterm birth and mortality and morbidity: a population-based quasi-experimental study. JAMA Psychiatry 70, 1231–2140.

Dubois, J., Dehaene-Lambertz, G., Perrin, M., Mangin, J.F., Cointepas, Y., Duchesnay, E., Le Bihan, D., Hertz-Pannier, L., 2008. Asynchrony of the early maturation of white matter bundles in healthy infants: quantitative landmarks revealed noninvasively by diffusion tensor imaging. Hum. Brain Mapp. 29, 14–27.

Eaton-Rosen, Z., Melbourne, A., Orasanu, E., Modat, M., Cardoso, M.J., Bainbridge, A., Kendall, G.S., Robertson, N.J., Marlow, N., Ourselin, S., 2014. Longitudinal measurement of the developing thalamus in the preterm brain using multi-modal MRI. Med. Image Comput. Comput. Assist. Interv. 8674, 276–283.

Ferguson, B.R., Gao, W.J., 2015. Development of thalamocortical connections between the mediodorsal thalamus and the prefrontal cortex and its implication in cognition. Front. Hum. Neurosci. 8.

Fischl, B., Salat, D.H., Busa, E., Albert, M., Dieterich, M., Haselgrove, C., van der Kouwe, A., Killiany, R., Kennedy, D., Klaveness, S., Montillo, A., Makris, N., Rosen, B., Dale, A.M., 2002. Whole brain segmentation: automated labeling of neuroanatomical structures in the human brain. Neuron 33, 341–355.

Gilmore, J.H., Feng, S., Woolson, S.L., Knickmeyer, R.C., Short, S.J., Lin, W., Zhu, H., Hamer, R.M., Styner, M., Shen, D., 2012. Longitudinal development of cortical and subcortical gray matter from birth to 2 years. Cereb. Cortex 22, 2478–2485.

Han, X., Xu, C., Braga-Neto, U., Prince, J.L., 2002. Topology correction in brain cortex segmentation using a multiscale, graph-based algorithm. IEEE Trans. Med. Imaging 21, 109–121.

Herrero, M.T., Barcia, C., Navarro, J.M., 2002. Functional anatomy of thalamus and basal ganglia. Childs Nerv. Syst. 18, 386–404.

Hill, J., Inder, T., Neil, J., Dierker, D., Harwell, J., Van Essen, D., 2010. Similar patterns of cortical expansion during human development and evolution. Proc. Natl. Acad. Sci. U. S. A. 107, 13135–13140.

Holland, D., Chang, L., Ernst, T.M., Curran, M., Buchthal, S.D., Alicata, D., Skranes, J., Johansen, H., Hernandez, A., Yamakawa, R., Kuperman, J.M., Dale, A.M., 2014. Structural growth trajectories and rates of change in the first 3 months of infant brain development. JAMA Neurol. 71, 1266–1274.

Huttenlocher, P.R., 1979. Synaptic density in human frontal cortex—developmental changes and effects of aging. Brain Res. 163, 195–205.

Huttenlocher, P.R., Dabholkar, A.S., 1997. Regional differences in synaptogenesis in human cerebral cortex. J. Comp. Neurol. 387, 167–178.

Jones, E.G., 1997. Cortical development and thalamic pathology in schizophrenia. Schizophr. Bull. 23, 483–501.

Joshi, S., Davis, B., Jomier, M., Gerig, G., 2004. Unbiased diffeomorphic atlas construction for computational anatomy. NeuroImage 23 (Suppl. 1), S151–S160.

Li, C.S., Huang, C., Constable, R.T., Sinha, R., 2006. Imaging response inhibition in a stop-signal task: neural correlates independent of signal monitoring and post-response processing. J. Neurosci. 26, 186–192.

Marlow, N., Wolke, D., Bracewell, M.A., Samara, M., 2005. Neurologic and developmental disability at six years of age after extremely preterm birth. N. Engl. J. Med. 352, 9–19.

Molfese, D.L., Freeman Jr., R.B., Palermo, D.S., 1975. The ontogeny of brain lateralization for speech and nonspeech stimuli. Brain Lang. 2, 356–368.

Please cite this article as: Poh, J.S., et al., Developmental synchrony of thalamocortical circuits in the neonatal brain, NeuroImage (2015), http://dx.doi.org/10.1016/j.neuroimage.2015.03.039

Mrzljak, L., Uylings, H.B.M., Kostovic, I., van Eden, C.G., 1988. Prenatal development of neurons in the human prefrontal cortex: I. A qualitative Golgi study. J. Comp. Neurol. 271, 355–386.
Nair, A., Treiber, J.M., Shukla, D.K., Shih, P., Müller, R., 2013. Impaired thalamocortical connectivity in autism spectrum disorder. Brain 136, 1942–1955.
Parker, G.J., Haroon, H.A., Wheeler-Kingshott, C.A., 2003. A framework for a streamline-based probabilistic index of connectivity (PICo) using a structural interpretation of MRI diffusion measurements. J. Magn. Reson. Imaging 18, 242–254.
Petanjek, Z., Judas, M., Kostovic, I., Uylings, H.B., 2008. Lifespan alterations of basal dendritic trees of pyramidal neurons in the human prefrontal cortex: a layer-specific pattern. Cereb. Cortex 18, 915–929.
Petanjek, Z., Judas, M., Simic, G., Rasin, M.R., Uylings, H.B., Rakic, P., Kostovic, I., 2011. Extraordinary neoteny of synaptic spines in the human prefrontal cortex. Proc. Natl. Acad. Sci. U. S. A. 108, 13281–13286.
Qiu, A., Fortier, M.V., Bai, J., Zhang, X., Chong, Y.S., Kwek, K., Saw, S.M., Godfrey, K.M., Gluckman, P.D., Meaney, M.J., 2013. Morphology and microstructure of subcortical structures at birth: a large-scale Asian neonatal neuroimaging study. NeuroImage 65, 315–323.
Sherman, S.M., 2007. The thalamus is more than just a relay. Curr. Opin. Neurobiol. 17, 417–422.
Sim, K., Cullen, T., Ongur, D., Heckers, S., 2006. Testing models of thalamic dysfunction in schizophrenia using neuroimaging. J. Neural Transm. 113, 907–928.
Smith, S.M., 2002. Fast robust automated brain extraction. Hum. Brain Mapp. 17, 143–155.
Soh, S.E., Tint, M.T., Gluckman, P.D., Godfrey, K.M., Rifkin-Graboi, A., Chan, Y.H., Stunkel, W., Holbrook, J.D., Kwek, K., Chong, Y.S., Saw, S.M., 2014. Cohort profile: Growing Up in Singapore Towards healthy Outcomes (GUSTO) birth cohort study. Int. J. Epidemiol. 43, 1401–1409.
Srinivasan, L., Dutta, R., Counsell, S.J., Allsop, J.M., Boardman, J.P., Rutherford, M.A., Edwards, A.D., 2007. Quantification of deep gray matter in preterm infants at term-equivalent age using manual volumetry of 3-tesla magnetic resonance images. Pediatrics 119, 759–765.
Tillman, C.M., Thorell, L.B., Brocki, K.C., Bohlin, G., 2008. Motor response inhibition and execution in the stop-signal task: development and relation to ADHD behaviors. Child Neuropsychol. 14, 42–59.
Van Essen, D.C., 1997. A tension-based theory of morphogenesis and compact wiring in the central nervous system. Nature 385, 313–318.
Van Ewijka, H., Heslenfelda, D.J., Zwiersc, M.P., Buitelaarc, J.K., Oosterlaana, J., 2012. Diffusion tensor imaging in attention deficit/hyperactivity disorder: a systematic review and meta-analysis. Neurosci. Biobehav. Rev. 36, 1093–1106.
Woodward, N.D., Karbasforoushan, H., Heckers, S., 2012. Thalamocortical dysconnectivity in schizophrenia. Am. J. Psychiatr. 169, 1092–1099.
Zhong, J., Qiu, A., 2010. Multi-manifold diffeomorphic metric mapping for aligning cortical hemispheric surfaces. NeuroImage 49, 355–365.
Zhong, J., Rifkin-Graboi, A., Ta, A.T., Yap, K.L., Chuang, K.H., Meaney, M.J., Qiu, A., 2014. Functional networks in parallel with cortical development associate with executive functions in children. Cereb. Cortex **24**, 1937–1947.

Please cite this article as: Poh, J.S., et al., Developmental synchrony of thalamocortical circuits in the neonatal brain, NeuroImage (2015), http://dx.doi.org/10.1016/j.neuroimage.2015.03.039